



**HAL**  
open science

# Mitigation of Water Management in PEM Fuel Cell Cathodes by Hydrophilic Wicking Microporous Layers

Ruediger Schweiss, Marcus Steeb, Peter M. Wilde

► **To cite this version:**

Ruediger Schweiss, Marcus Steeb, Peter M. Wilde. Mitigation of Water Management in PEM Fuel Cell Cathodes by Hydrophilic Wicking Microporous Layers. *Fuel Cells*, 2010, 10 (6), pp.1176. 10.1002/fuce.201000003 . hal-00576975

**HAL Id: hal-00576975**

**<https://hal.science/hal-00576975>**

Submitted on 16 Mar 2011

**HAL** is a multi-disciplinary open access archive for the deposit and dissemination of scientific research documents, whether they are published or not. The documents may come from teaching and research institutions in France or abroad, or from public or private research centers.

L'archive ouverte pluridisciplinaire **HAL**, est destinée au dépôt et à la diffusion de documents scientifiques de niveau recherche, publiés ou non, émanant des établissements d'enseignement et de recherche français ou étrangers, des laboratoires publics ou privés.



## Mitigation of Water Management in PEM Fuel Cell Cathodes by Hydrophilic Wicking Microporous Layers

Journal:	<i>Fuel Cells</i>
Manuscript ID:	fuce.201000003.R1
Wiley - Manuscript type:	Communication
Date Submitted by the Author:	22-Jun-2010
Complete List of Authors:	Schweiss, Ruediger; SGL Technologies GmbH Steeb, Marcus; SGL Technologies GmbH Wilde, Peter; SGL Technologies GmbH
Keywords:	PEM Fuel Cell, Water Management, Gas Diffusion Electrode, microporous layer, Performance

SCHOLARONE™  
Manuscripts

# Mitigation of Water Management in PEM Fuel Cell Cathodes by Hydrophilic Wicking Microporous Layers

Rüdiger Schweiss\*, Marcus Steeb, Peter M. Wilde

SGL Technologies GmbH  
Werner-von-Siemens-Strasse 18  
DE-86405 Meitingen, Germany  
Phone +49 8271 831702  
[ruediger-bernd.schweiss@sglcarbon.de](mailto:ruediger-bernd.schweiss@sglcarbon.de)

## Abstract

This study introduces a novel strategy for enhancing the performance of Polymer Electrolyte Fuel Cells at high current densities by means of an advanced gas diffusion layer design. The incorporation of hydrophilic wicking agents into microporous layers of the cathode gas diffusion layer improves water management, thus increasing the maximum power density of Polymer Electrolyte Fuel Cells. *Ex-situ* measurements with respect to water and vapour transport, and electrochemical polarisation data provide evidence suggesting that the beneficial effect has to be attributed to enhanced liquid water removal through the microporous layer.

**Keywords:** PEMFC, water management, gas diffusion layer, microporous layers

## 1 Introduction

Polymer electrolyte fuel cells (PEMFCs) constitute promising candidates for future energy systems which will have to pay particular attention to carbon footprint and efficiency. Such requirements are fulfilled by fuel cells which enable a direct conversion of fuel into electrochemical power while only releasing non-toxic effluents from the system. Forthcoming applications are mainly seen in the field of automotive propulsion or backup power. In order to substitute fossil fuel systems, the PEMFC still has to overcome barriers relating to costs and infrastructure and also has to address technical aspects such as durability and performance (which are, in turn, related to costs).

Among the technical issues, water management is one of the critical processes in the operation of Polymer Electrolyte Fuel Cells (PEMFCs) [1,2]. Especially in the case of high current density applications such as automotive PEM stacks, mass-transport limitation due to water accumulation is the predominant factor limiting stack performance. In this context, a complex interplay of different competing processes of water generation, water removal, water evaporation, water condensation, and water transport (in the liquid or gas phase) has to be controlled by means of system design, operation mode or fuel cell component properties. From the membrane perspective, a high level of hydration has to be maintained, whereas for the porous media such as the catalyst sites, the gas diffusion layers and the flowfield backings, an efficient removal of liquid water is indispensable. Additionally, the excess water in the porous media not only affects the performance, but also has implications on the degradation of functional components and is further associated with critical events during freeze shutdown/startup of PEMFC stacks [3].

At the component level, different approaches to controlling water transport and removing water from PEMFCs have been described in literature, such as MEA design [3], control of hydrophilicity and microstructure of flow fields [4,5] or the insertion of a water management layer [6].

As the interface between the active areas and the flowfield backing, the gas diffusion layers (GDLs) are not only the key moderators for the different water transport phenomena but also, apart from the flowfields, the main site of water accumulation. Gas diffusion layers which consist of porous carbon fibre webs (papers, nonwovens or cloths) are commonly treated with fluoropolymers and coated with a microporous layer (MPL) in order to perform the complex task of maintaining a certain humidification level of the adjacent catalyst sites and the membrane while avoiding flooding of its porous body which would compromise the reactand gas supply. Additionally, it has been reported that the electroosmotic drag is also influenced by GDL characteristics. At high humidification levels, the use of a GDL with a hydrophobised base substrate and a microporous layer is common practice [7-9]. Water saturation in the GDL was observed to decrease when an MPL is present [8, 10]. Additionally, the in-plane permeability of a GDL without an MPL is much larger and thus leads to an increased

1  
2  
3 pressure drop which is unfavorable for water removal [11]. Excessive loading of the GDL and the MPL with  
4 fluoropolymer, however, was shown to induce flooding of the catalyst layers.

5 A number of studies were recently conducted based on computer modelling approaches or in-situ water imaging  
6 with x-ray or neutron radiography in order to arrive at a deeper understanding of the mechanisms underlying  
7 water transport in GDLs [12].

8 A simple description based on capillary-driven flow only was concluded to be insufficient to predict liquid water  
9 transport in porous diffusion media, because in this case continuous liquid water flow from the site of high  
10 saturation to the areas of lower water saturation would occur [13]. This is why continuous water flow has never  
11 been observed in practice.

12 These findings are supported by water imaging with fluorescent dyes [14], which show that water transport in  
13 hydrophobic GDLs is determined by a capillary fingering mechanism with only a few clusters that are released  
14 more or less periodically (also referred to as “eruptions” [15,16]).

15 Theoretical considerations taking into account vapour diffusion and thermal gradients across the GDL under real  
16 operating conditions suggest, that for an hydrophobic MPL-coated GDL, the majority of the excess water is  
17 transported in the vapour phase [17]. This is supported by Synchrotron x-ray radiography studies by Hartnig *et*  
18 *al.* [18], who showed that water is formed primarily near the channel ribs of the flow field and that, regardless of  
19 the current density, hardly any liquid water is present in the microporous layers. Two diffusion barriers were  
20 found to be located at the MPL/GDL substrate-interface and at the catalyst-MPL boundary. Neutron imaging  
21 similarly yields indications that water is accumulated at the landings and the channel bends [11, 19].  
22

23 The current picture of water transport in porous, hydrophobic gas diffusion media is therefore that

- 24 • the liquid water condensation is dependent on the local wettability and the temperature gradient in the  
25 GDL
- 26 • a branched water profile with a certain fraction of dead ends exists in the GDL substrate
- 27 • there are preferential pathways of liquid water removal that evolve over time
- 28 • the content of liquid water in the MPL is low
- 29 • water release from the GDL is described by an eruptive mechanism.  
30  
31  
32

33 As a result, advanced GDL designs will have to go beyond the simple wet-proofing approach and advance  
34 towards an “engineered porosity/hydrophobicity” [20]. In this context, water flow analyses suggest that a  
35 bimodal pore size distribution might be an advanced GDL design principle [21].

36 As a step towards controlled hydrophilic/hydrophobic porosity, this paper introduces a novel strategy of water  
37 management mitigation in PEM fuel cells by means of enhancing liquid water transport through the microporous  
38 layer of the cathode GDL. This is accomplished by the incorporation of hydrophilic fibres in the microporous  
39 layers which act as pathways of preferential liquid water flow. A parametric study was conducted with several  
40 reference materials, the emphasis being placed on ex-situ water transport and in-situ measurements.  
41

## 42 2 Experimental

### 43 2.1 GDL substrates

44  
45 **Rolls of Sigracet® Gas Diffusion Layers GDL** (carbon paper grades 24 AA, 25 AA), SGL Technologies  
46 GmbH, Meitingen, Germany) were treated with aqueous polytetrafluoroethylene (PTFE) dispersion by means of  
47 a dipping process in order to obtain a 5% (w/w) PTFE load of the substrates [22]. The hydrophobised substrates  
48 (designated as 24 BA and 25 BA) had open porosities of 89% (25 BA, 35 BA) and 84% (24 BA, 34 BA). The  
49 low porosity GDL are therefore recommended for dry operation whereas the highest performance is generally  
50 obtained using 25 BC at high humidification levels [23, 24].  
51  
52

### 53 2.2 Microporous Layers

54  
55 Chopped aluminosilicate fibres (type ALTRA B97 LA C25, Rath GmbH, Mönchengladbach, Germany, fibre  
56 diameter 2-4 µm) were treated in a ball mill (Fritsch, Idar-Oberstein, Germany) for 2 mins. The milled fibres  
57 obtained had lengths from 20-90 µm( determined by laser diffraction). Thereafter, they were dispersed in  
58 deionized water (10 g in 100 g water)

59 The fibre dispersion was added to an aqueous dispersion of acetylene black and PTFE in order to obtain coating  
60 paste with a carbon to fibre ratio of 10:1. The paste was applied to a GDL substrate using a continuous blade  
coating line. This procedure yields a GDL designated as 25 BL. The C-type MPLs (24 BC and 25 BC materials)  
were prepared accordingly without addition of aluminosilicate fibres. All MPLs (L and C) had a carbon to PTFE  
ratio of 77:23. Next, the coated GDLs were subjected to a sintering process at 350°C for 10 minutes.

## 2.3 Characterization

The GDLs were characterised with regard to electrical properties, porosity, gas permeability, water vapour transmission and liquid permeability [22,23]. Capillary flow porometry (CFP) was performed with a PMI capillary flow porometer (Porous Materials Inc, USA) and liquid permeability was carried out by means of a PMI liquid permeability tester (Porous Materials Inc, USA). Gas permeability was determined using the Gurley method (TAPPI T460, 304 Pa). Water vapour transmission (according to ASTM D6701-01) of GDLs was measured with a Mocon Permatran-W 101K Setup (Mocon Inc, Minneapolis, USA). Single-cell fuel cell tests were performed on a Fuel cell test bench (Hydrogenics Corp Burnaby, CA) using a pneumatically sealed test cell with an active area of 25 cm<sup>2</sup> (Baltic Fuel Cells, Schwerin, Germany). A commercial CCM (Primea 5710®, 0.4 mg cm<sup>-2</sup> Pt on cathode, 0.1 mg cm<sup>-2</sup> Pt on the anode side, WL Gore Associates, Putzbrunn, Germany) was sandwiched between anodic and cathodic GDLs facing graphite flow fields at a compression load of 1 N mm<sup>-2</sup>. Stoichiometry was 1.52 on the anode and 2.50 on the cathode, respectively. Inlet pressure was 50 kPa. Sigracet® 25 BC was used as a standard anode GDL for all of the experiments.

## 3 Results and Discussion

Figure 1 shows micrographs of the surface of an MPL with embedded aluminosilicate fibres (GDL 25 BL). Given the total amount of fibres in the MPL and comparing them to microscopic images of several larger MPL areas, it can be concluded that most of the fibres are buried beneath the top surface where they can act as hydrophilic wicks in the microporous layer. Mud cracks were observed for both substrates, but the overall frequency of mud cracks was not found to differ noticeably for both MPLs.

### 3.1 Pore Characteristics

Pore size distribution was determined using capillary flow porometry [24, 25]. Figure 2 shows the flow pore size distribution of different GDLs. Despite the fact that all of the GDLs were coated with the same microporous layer formulation, it was observed that the pore size distribution is still significantly influenced by the GDL base substrate. The GDL based on substrates with the lower porosity (24 BC) consequently shows a mean pore diameter less than GDLs with the 25 base substrate. The addition of hydrophilic fibres to the MPL, in turn, does not have any noticeable effect on the pore size distribution, but only results in a slightly larger bubble point (25 BC = 32 μm, 25 BL = 34 μm).

### 3.2 Gas, liquid water and water vapour transport properties

Figure 2 shows a water vapour transmission measurements of GDL reference materials with different substrate thickness and porosity and a standard MPL (C) and the novel GDL with a modified MPL (25 BL). The water vapour transmission is primarily determined by the diffusion length (GDL thickness) and to a lesser extent by the substrate porosity (as seen by the values obtained for 24/25 and 34/35, respectively). By contrast, no significant effect of the MPL composition on the vapor diffusion was observed.

Since liquid water transport is assumed to be driven by hydraulic pressure [13], liquid permeability measurements [7] of the GDLs were carried out. As revealed in Figure 4, 25 BL shows a much higher liquid water flux at a given pressure than the 25 BC GDL. This cannot be attributed to differences in the MPL porosity, but is solely the consequence of the hydrophilic wicking effect which is due to the presence of the inorganic fibres. The resistance of the 25 BL against liquid water transport is therefore reduced by factor 5 as compared to the 25 BC. The onset of the flow curve (also referred to as hydrohead pressure [7] which is the intercept at flux = 0), however, is very similar for both GDLs (0.12 kPa for 25 BL and 0.2 kPa for 25 BC). This means that there are no significant differences in capillary pressure for both GDLs. In other words, the MPL matrix of 25 BL is clearly hydrophobic and the liquid water transport predominantly occurs along a network formed by the hydrophilic fibres.

### 3.2 Fuel Cell Tests

Single-cell fuel cell tests on the different GDL substrates on the cathode side (25 BC was used as a reference on the anode) are depicted in Figure 3. Electrochemical polarisation curves at two different temperatures and humidification levels show distinct differences in the GDL properties. As expected, the low porosity gas diffusion layer (24 BC) shows a mass transport limitation at current densities of more than 0.6 and 1 A cm<sup>-2</sup>, respectively. Especially under high humidity conditions (60°C, 100% RH, high current density), the GDL with hydrophilic constituents (25 BL) displays a beneficial effect corresponding to an approximately 8% increase in maximum power as compared to 25 BC. This means that, the 25 BL cathode diffusion layer obviously removes excess water more efficiently than the reference systems. This is due to enhanced water transport in the liquid phase which is caused by the aforementioned hydrophilic wicking mechanism. Interestingly, cathodes based on 25 BL also show a higher power than 25 BC under dry conditions (40% RH) which might be due to the fact that it could retain more liquid water as compared to the 25 BC under low water saturation (dry) conditions.

### Conclusions

Gas diffusion media with different properties such as porosity and hydrophobicity were characterised with regard to different water transport mechanisms. A novel concept for tailoring the degree of hydrophilicity of the microporous layer shows a beneficial effect on the water management of cathode GDLs. This is verified by *ex-situ* methods and single-cell fuel cell studies. The increased performance of the novel MPL with hydrophilic wicks demonstrates that a gas diffusion layer with enhanced liquid water permeability is capable of retarding the flooding of the catalyst sites under wet conditions. The beneficial effect of hydrophilic constituents in the microporous layers is twofold. Firstly, an enhanced lateral diffusion of water at the catalyst-MPL interface is expected to counteract excessive flooding of the active areas. Secondly, preferential pathways are generated to guide liquid water through the microporous layers. Evidence of the mechanism is provided by *ex-situ* water transport measurements and single-cell tests. Further insights into the water transport mechanisms of the different GDLs types are expected from in-situ neutron imaging studies which are currently being performed [26].

In summary, it has been verified that even the addition of hydrophilic compounds to the microporous layer in a relatively arbitrary fashion does indeed improve water management in a fuel cell. In line with a recent study by Park *et al.* [27], this study also stresses the importance of a liquid water transport properties of gas diffusions layers for fast drainage and fuel cell performance.

Water management can be expected to be further improved by the locally controlled placement of hydrophilic patterns, taking into account the specific flow field geometries.

### Acknowledgment

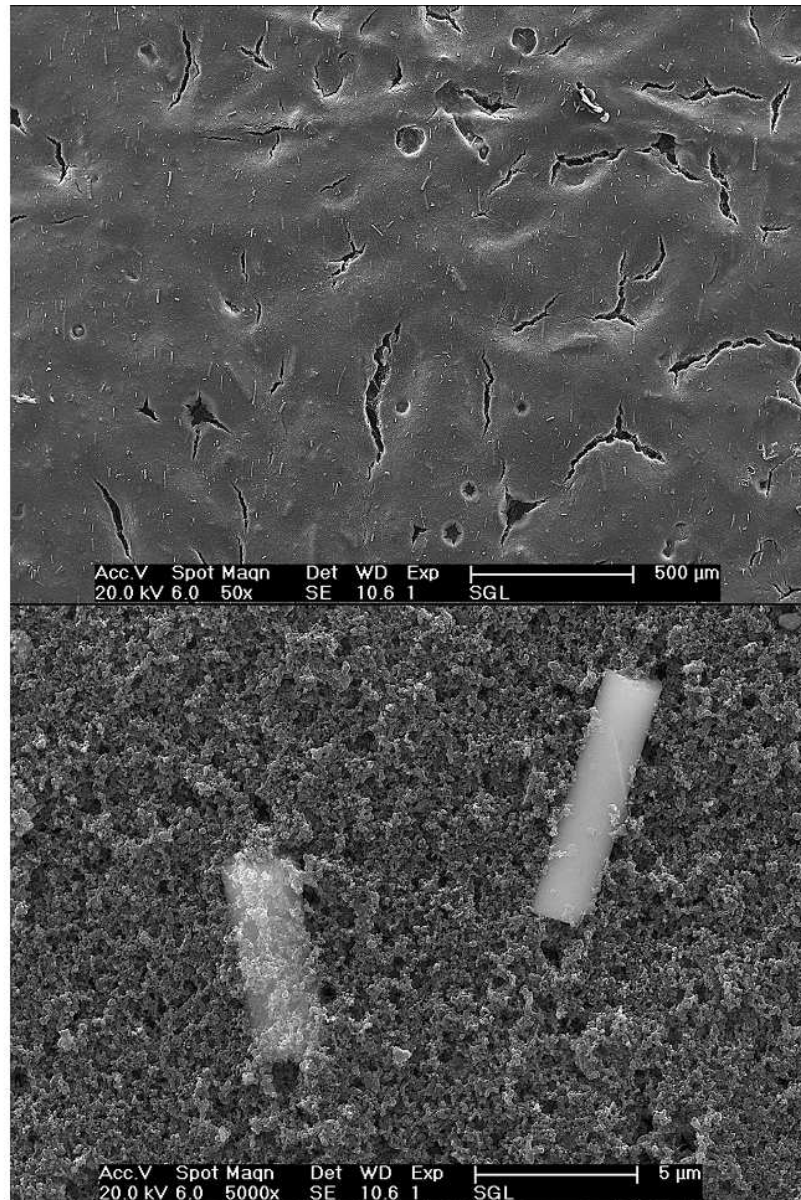
The authors would like to express their gratitude to Werner Buergel for SEM images and to Stefan Woehner (SGL Group, Meitingen) for providing liquid permeability measurements.

### References

- [1] J. P. Meyers in F. N. Büchi, M. Inaba, T. J. Schmidt (Eds.) *Polymer Electrolyte Fuel Cell Durability*, Springer, New York, 2009.
- [2] H. Li, Y. Tang, Z. Wang, Z. Shi, S. Wu, D. Song, K. Zhang, K. Fatih, J. Zhang, H. Wang, Z. Liu, R. Abouatallah, A. Mazza, *J. Power Sources* **2008**, 178, 103.
- [3] J. St.-Pierre, D. P. Wilkinson, S. Knights, M. Bos. *J. New Mater. Electrochem. Syst.* **2000**, 3, 99.
- [4] T. Metz, N. Paust, C. Müller, R. Zengerle, P. Koltay. *Sens. Actuators* **2008**, 143, 49.
- [5] J. Chen, T. Matsuura, M. Hori. *J. Power Sources* **2004**, 131, 155.
- [6] L. Cindrella, A. M. Kannan, J. F. Lin, K. Saminathan, Y. Ho, C. W. Lin, J. Wertz, *J. Power Sources* **2009**, 194, 146.
- [7] M. F. Mathias, J. Roth, J. Fleming, W. Lehnert in W. Vielstich, H. A. Gasteiger, A. Lamm (Eds.) *Handbook of Fuel Cells – Fundamentals Technology and Applications*, Vol. 3, Wiley, New York, **2003**, Chapter 46
- [8] J. T. Gostick, M. A. Yoannidis, M. W. Fowler, M. D. Pritzker, *J. Power Sources* **2009**, 194, 433.
- [9] J. T. Gostick, M. A. Yoannidis, M. W. Fowler, M. D. Pritzker, *Electrochem. Comm.* **2009**, 11, 576.
- [10] A. Z. Weber, J. Newman, *J. Electrochem. Soc.* **2005**, 152, 677.
- [11] J. P. Owejan, T. A. Trabold, D. L. Jacobsen, M. Arif, S. G. Kandlikar, *Int. J. Hydrogen Energy* **2007**, 32, 4489

- 1  
2  
3 [12] A. Bazylak, *Intl. J. Hydrogen Energy* **2009**, *34*, 3845-3857  
4 [13] P. Zhou, C. W. Wu, *J. Power Sources* **2010**, *195*, 1408  
5 [14] U. Pasaogullari, C. Y. Wang, *J. Electrochem Soc.* **2004**, *151*, A399.  
6 [15] S. Litster, D. Sinton, N. Djilali, *J. Power Sources* **2006**, *154*, 95.  
7 [16] F.Y. Wang, X. G. Yang, C. Y. Wang, *J. Electrochem. Soc.* **2006**, *153*, A225.  
8 [17] S. F. Burlatsky, V. V. Athrazev, M. Gummalla, D. A. Condit, F. Lui, *J. Power Sources* **2009**, *190*, 485.  
9 [18] Ch. Hartnig, I. Mahnke, R. Kuhn, N. Kardjilov, J. Banhart, W. Lehnert, *Appl. Phys. Lett.* **2008**, *92*,  
10 134106.  
11 [19] R. Mukundan, R. L. Borup, *Fuel Cells* **2009**, *5*, 499.  
12 [20] P.K. Sinha, C. Y. Wang, *Chem. Eng. Sci.* **2008**, *63*, 1081.  
13 [21] J. Benziger, J. Nehlsen, D. Blackwell, T. Brennan, J. Itescu, *J. Membr. Sci.* **2005**, *261*, 98.  
14 [22] P. M. Wilde, M. Mändle, M. Murata, N. Berg, *Fuel Cells* **2004**, *4*, 180.  
15 [23] T. Kitahara, T. Konomi, M. Murata, N. Berg, P. Wilde, *ECS Trans.* **2007**, *5*, 27  
16 [24] T. Kitahara, T. Konomi, H. Nakajima, Y. Tateishi, M. Murata, N. Haak, P. Wilde, *ECS Trans.* **2008**, *16*,  
17 1603  
18 [25] A. Jena, K. Gupta, *41st Power Sources Conference*, **2004**. www.pmiapp.com  
19 [26] R. Mukundan et al., *in preparation*  
20 [27] S. Park, B.N. Popov, *Fuel* **2009**, *88*, 2068.  
21  
22  
23  
24  
25  
26  
27  
28  
29  
30  
31  
32  
33  
34  
35  
36  
37  
38  
39  
40  
41  
42  
43  
44  
45  
46  
47  
48  
49  
50  
51  
52  
53  
54  
55  
56  
57  
58  
59  
60

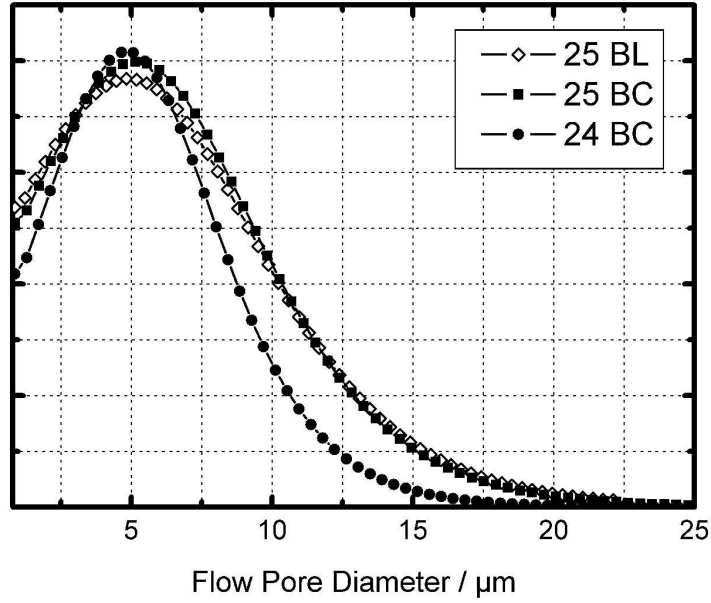




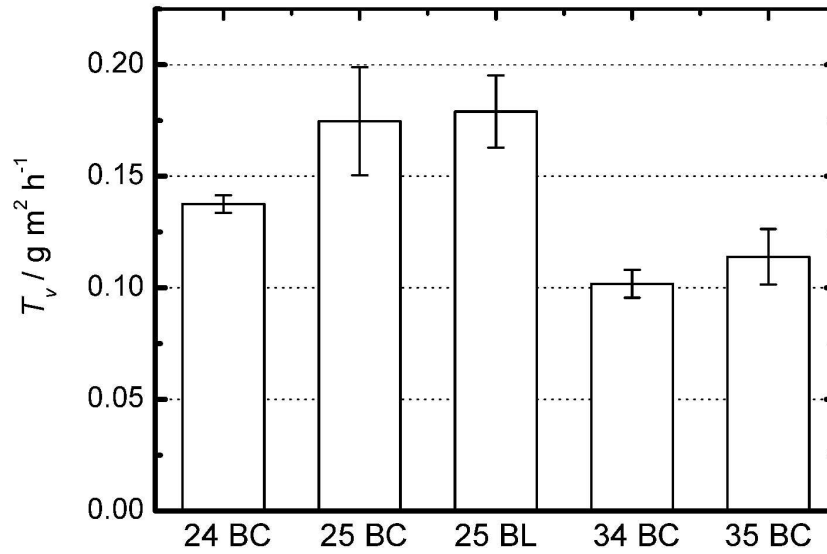
SEM images of a microporous layer with incorporated hydrophilic fibres  
190x255mm (96 x 96 DPI)



1  
2  
3  
4  
5  
6  
7  
8  
9  
10  
11  
12  
13  
14  
15  
16  
17  
18  
19  
20  
21  
22  
23  
24  
25  
26  
27  
28  
29  
30  
31  
32  
33  
34  
35  
36  
37  
38  
39  
40  
41  
42  
43  
44  
45  
46  
47  
48  
49  
50  
51  
52  
53  
54  
55  
56  
57  
58  
59  
60

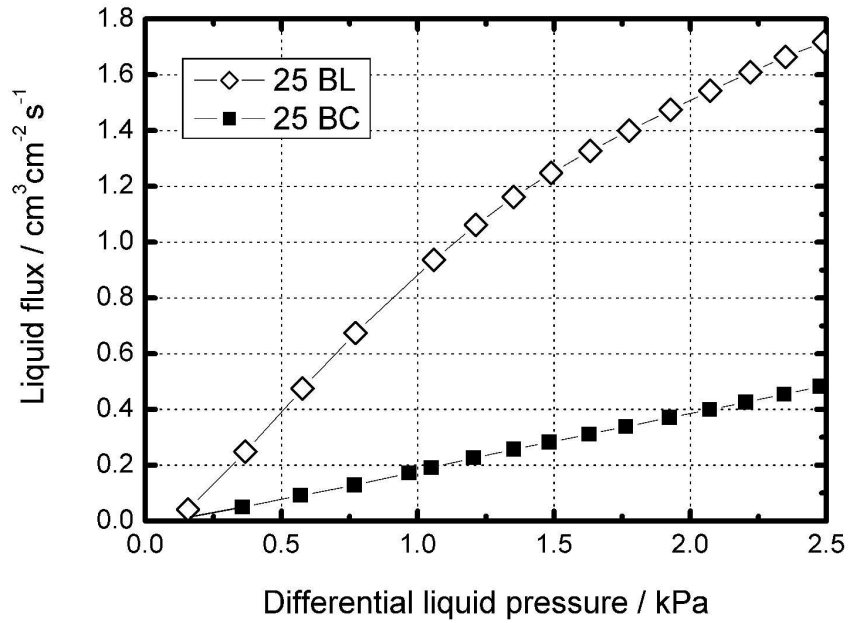


Pore size distribution of the GDLs as calculated based on capillary flow measurements (averages of 3 runs)  
288x201mm (300 x 300 DPI)



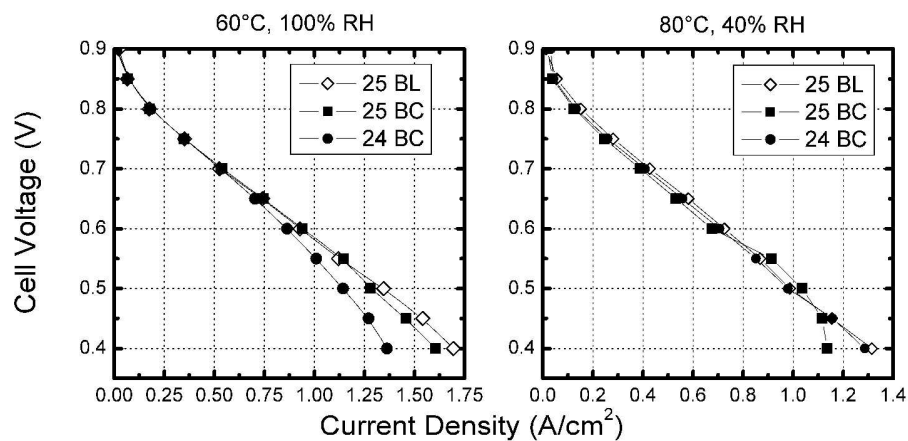
Water vapour transmission of GDL reference material and GDL 25 BL.  
288x201mm (300 x 300 DPI)

1  
2  
3  
4  
5  
6  
7  
8  
9  
10  
11  
12  
13  
14  
15  
16  
17  
18  
19  
20  
21  
22  
23  
24  
25  
26  
27  
28  
29  
30  
31  
32  
33  
34  
35  
36  
37  
38  
39  
40  
41  
42  
43  
44  
45  
46  
47  
48  
49  
50  
51  
52  
53  
54  
55  
56  
57  
58  
59  
60



Comparison of liquid water permeability measurements for 25 BC and 25 BL  
288x201mm (300 x 300 DPI)

Review



Electrochemical polarisation curves of single cells with different cathode GDLs under wet conditions (60°C, 100% RH) and dry conditions (80°C, 40% RH). GDL 25 BC was used as standard on the anode.

406x177mm (300 x 300 DPI)